Bounds on the complex viscoelasticity for ocean wave propagation in the marginal ice zone

C. Sampson, N. B. Murphy, E. Cherkaev, and K. M. Golden

The propagation of ocean surface waves through the polar sea ice covers is a critical process in Earths climate system. In models which consider the ocean surface layer to be a composite of ice floes and water characterized rheologically in the long wavelength regime by its effective complex viscoelasticity, this key parameter has only been fitted to wave data. Here we present the first rigorous bounds on the homogenized viscoelasticity by deriving a Stieltjes integral representation for it, involving a spectral measure which depends on the geometry of ice floe configurations.

INTRODUCTION

The marginal ice zone (MIZ) is the region of sea ice cover that is close enough to the open ocean to be affected by its dynamics. Over the past several years there has been an increasing realization of the importance of wave-ice interactions in the growth and decay of the seasonal ice pack. In fact, a striking correlation between Antarctic sea ice extent and wave activity has been found recently [13]. In both the Arctic and Antarctic, the ice floe size distribution in the MIZ plays a central role in the properties of wave propagation though it. Ocean waves break up and shape the ice floes which, in turn, attenuate various wave characteristics, controlling which wave magnitudes and wavelengths propagate further into the pack. This ice-ocean interaction has become increasingly important recently in the Arctic, due to the dramatic decrease of the summer ice extent which has increased the size of the Arctic MIZ. These recent changes in the Arctic may promote more rapid ice loss and incease shore errosion effecting the Arctic inhabitants. It is therefore paramount that wave ice interactions, which are complex and often numerically expensive to incorporate into models, be accurately accounted for. Recently, continuum models have been developed which treat the MIZ as a two component composite of ice and slushy water. Several of the proposed models treat the ice and slushy water mix as a single material atop an inviscid ocean. These models are particularly appropriate for longer wavelengths. The top layer has been taken to be purely elastic [1], purely viscous [12], and viscoelastic [17, 25]. At the heart of these models are effective parameters, namely, the effective elasticity, viscosity, and complex viscoelasticity. In practice, these effective parameters, which depend on the composite geometry and the physical properties of the constituents, are quite difficult to determine. To help overcome this limitation, we employ the methods of homogenization theory, in a quasi-static, fixed frequency regime, to find a Stieltjes integral representation for the complex viscoelasticity of the two layer model presented in [25], a model already being incorporated into Wave Watch III. We choose this model as it is a more general case which can be reduced to the purely viscous or purely elastic cases. The derivation is motivated by earlier work in [7]. There a Stieltjes integral representation is derived for a compressible viscoelastic material. The analytic Stieltjes integral representation has been extended to effective elastic properties in the past as well [6, 8, 16, 20]. Stieltjes integral representations for the effective viscoelastic shear modulus have been previously obtained using the torsion of a viscoelastic cylinder whose microstructure is uniform in the axial direction [3, 4, 22]. The integral representation we find involves the spectral measure of a self adjoint operator and provides bounds on the effective viscoelasticity using the analytic continuation method [2, 10, 15]. The bounds themselves depend on the moments of the measure: the more moments known, the tighter the bounds. We further develop a simple wave equation which governs wave motion in the quasi-static regime. This equation produces a simplified dispersion relation that relates the wave number and attenuation rate of plane like waves traveling through the MIZ to the effective parameter. We then use the wave equation to model wave breaking of ice in the MIZ and are able to accurately capture many average characteristics of the floe size distribution in the marginal ice zone of Antarctica.

MATHEMATICAL METHODS

In linear elasticity theory the stress σ is related to the strain ϵ through a fourth rank tensor C via the relation $\sigma = C : \epsilon$ where : is contraction. In the static case the effective elasticity tensor for a linearly elastic material can be defined as the tensor that relates the average stress to the average strain.

$$\langle \sigma \rangle = \langle C : \epsilon \rangle = C^* : \langle \epsilon \rangle \,. \tag{1}$$

Here σ and ϵ are stationary random fields and $\langle \cdot \rangle$ denotes spatial average. This corresponds to an average over all possible realizations of σ and ϵ.

In [25], the ice-slush composite is modeled as a Kelvin-Voight material for which the deviatoric part of the stress tensor is given by $\sigma_{ij} = 2G\epsilon_{ij} + 2\upsilon_{ij}\rho_1\dot{\epsilon}_{ij}$, where $\epsilon_{ij} = (1/2)(\nabla u + \nabla^T u) = \nabla^S u$ is the strain tensor, G the shear modulus, and υ the viscosity. Here u is the displacement and if we consider a harmonic wave profile, $u \approx \exp(kx -$

$i\omega t$) we see that $\dot{\epsilon}_{ij} = -i\omega\epsilon_{ij}$. Under this time harmonic assumption we may then write the deviatoric part of the stress tensor as $\sigma_{ij} = 2(G - i\omega\rho_1 v)\epsilon_{ij} = 2\nu\epsilon_{ij}$. In this case the momentum equation of the ice layer is given by,

$$\rho_1 \partial_{tt} u = \nabla \cdot (\sigma + PI) - \rho_1 g e_z \,, \tag{2}$$

where I is the identity matrix. We further take the material to be incompressible and irrotational, satisfying $\nabla \cdot u = 0$ and $\nabla \times \epsilon = 0$. From the definition of the deviatoric part of the stress tensor above we further see that we have two constitutive relationships namely, $\sigma = 2\nu\epsilon$ and $\epsilon = (1/2\nu)\sigma$.

For the boundary conditions in [25], when $\omega << 1$ and $k_r << 1$ it can be shown that [**?**]

$$\nabla \cdot PI \approx \rho_1 g e_z \,. \tag{3}$$

Further, we take only frequencies where $\omega^2 << 1$ so that $\partial_{tt} u = -i\omega^2 u \approx 0$. In this limit we obtain our quasi-static and irrotational set of governing equations together with two constitutive equations

$$\nabla \cdot \sigma = 0 \,, \qquad \sigma = 2\nu\epsilon \,, \tag{4}$$

$$\nabla \times \epsilon = 0 \,, \qquad \epsilon = \frac{1}{2\nu}\sigma \,. \tag{5}$$

At this point we now define two fourth rank tensors, $C = 2\nu\Lambda_s$ and $L = (1/2\nu)\Lambda_s$ where $\Lambda_s = (1/2)(\delta_{ik}\delta_{jl} + \delta_{il}\delta_{jk} - (1/d)\delta_{ij}\delta_{kl})$ is a projection on to the space of trace free rank two tensors [7, 23]. With these definitions we can then define the effective elasticity and compliance tensors through the equations,

$$\langle\sigma\rangle = \langle C : \epsilon\rangle = C^* : \langle\epsilon\rangle = 2\nu^*\epsilon_0 \,, \tag{6}$$

$$\langle\epsilon\rangle = \langle L : \sigma\rangle = L^* : \langle\sigma\rangle = \frac{1}{2\nu^*}\sigma_0. \tag{7}$$

INTEGRAL REPRESENTATION

Consider a two phase composite composed of materials with complex viscoelasticities ν_1, ν_2. We may then take our elasticity and compliance tensors to be $C = 2(\chi_1\nu_1 + \chi_2\nu_2)\Lambda_s$ and $L = (1/2)(\chi_1\nu_1^{-1} + \chi_2\nu_2^{-1})$ where χ_i is the characteristic function which takes on value 1 in material i and 0 otherwise. We may then substitute these into 4 while defining $\epsilon = \epsilon_0 + \epsilon_f$ and $\sigma = \sigma_0 + \sigma_f$ where ϵ_f and σ_f are the zero mean fluctuations around the average strain and stress ϵ_0 and σ_0 respectively. This leads to the following resolvent formulas for the stress and the strain,

$$\epsilon = \left(1 - \frac{1}{s}\Gamma\chi_1\right)^{-1}\epsilon_0, \quad \Gamma = \nabla^s(\nabla\cdot\nabla^s)^{-1}\nabla\cdot \,, \tag{8}$$

$$\sigma = \left(1 - \frac{1}{s}\Upsilon\chi_2\right)^{-1}\sigma_0, \quad \Upsilon = \nabla\times(\nabla\times\nabla\times)^{-1}\nabla\times \,. \tag{9}$$

Defining the inner product $\langle f, g\rangle = \langle f : \bar{g}\rangle$, and associated norm $||f|| = \sqrt{\langle f, f\rangle}$, we can then employ the spectral theorem to obtain the following Stieltjes integral representations 10 for the effective viscoelasticity,

$$\frac{\nu^*}{\nu_2} = ||\epsilon_0||^2(I - F(s)) \,, \qquad F(s) = \int_0^1 \frac{d\mu(\lambda)}{s-\lambda} \tag{10}$$

$$\frac{\nu_1}{\nu^*} = ||\sigma_0||^2 (I - E(s)) \,, \qquad E(s) = \int_0^1 \frac{d\eta(\lambda)}{s-\lambda} \tag{11}$$

RIGOROUS BOUNDS

While these integral representations are exact, the measures μ, η are difficult to calculate however insight on the effective parameter can be obtained through knowledge of their moments, which can be calculated using assumptions about the geometry of the composite. Bounds on ν^* can be obtained for a fixed contrast parameter s and are determined by varying over admissible measures μ, η with have moments matching those derived from geometric assumptions. Thus, this is the equivalent to varying over admissible geometries of the composite material. The more moments known, the tighter the bounds [9, 18]. For the elementary bounds, knowledge of only the masses of the measures μ_0, η_0 are required and is easily calculated using (12),

$$\mu^n = \int_0^1 \lambda^n d\mu(\lambda) = \langle(\chi_1\Gamma\chi_1)^n\chi_1\hat{\epsilon}_0 : \hat{\epsilon}_0\rangle \,, \tag{12}$$

$$\eta^n = \int_0^1 \lambda^n d\eta(\lambda) = \langle(\chi_2\Gamma\chi_2)^n\chi_2\hat{\sigma}_0 : \hat{\sigma}_0\rangle \,, \tag{13}$$

where $(\chi_1\Gamma\chi_1)^0 = I$, $\hat{\epsilon}_0 = \epsilon_0/||\epsilon_0||$, and $\hat{\sigma}_0 = \sigma_0/||\sigma_0||$, so that $\mu_0 = \langle\chi_1\rangle = p_1$ and $\eta_0 = \langle\chi_2\rangle = p_2$.

Following the procedure in [9, 18], we can show that ν^* must lie between the circles,

$$Q_0 = \nu_2\left(1 - \frac{p_1}{s-\lambda}\right) \,, \qquad 0 \le \lambda \le p_2 \tag{14}$$

$$\hat{Q}_0 = \frac{\nu_1}{1 - \frac{p_2}{s-\lambda}} \,, \qquad 0 \le \lambda \le p_1 \tag{15}$$

in the complex plane. We note that these are analogous to the elementary bounds in the electric case [9]. In order to calculate the bounds, knowledge of the component parameters $\nu_1 = G_1 - i\rho\omega\upsilon_1$ and $\nu_2 = G_2 - i\rho\omega\upsilon_2$ is needed. For the density we take the average of the densities between ice and water, $\rho \approx 974 kg/m^3$. Measurements of the shear modulus of first year ice have been made and suggest it is on the order of $G \approx 10^9 Pa$ [21]. Measurements of the viscosity of slush and grease ice suggest $\upsilon \approx 10^{-2} m^2/s$ [19, 24]. However, in the viscosity experiments elasticity is ignored. More recent wave tank experiments [26] show that a mix of mostly frazil ice, with some pancake ice, may have an effective viscoelastic parameter $\nu = G - i\rho\omega\upsilon$ with $G = 21Pa$ and $\upsilon = 0.014 m^2/s$

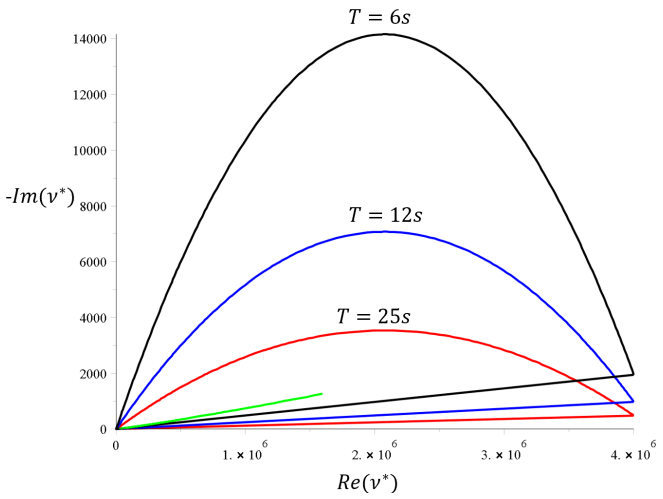

FIG. 1. The elementary bounds for wave periods of 25,12 and 6 S. As the period decreases, the bounds begin to be violated as we leave the quasi-static regime.

suggesting that there is some component of elasticity to be considered. One would be tempted to take the ice phase as purely elastic $\nu = G + 0i$. However, this would mean the ice is not lossy. In fact, ice attenuates waves much more strongly than the slush. This is due to scattering, and friction effects at the interface of the ice and water [14]. For our analysis we will take the slush to have parameters $G = 10Pa$ ad $\upsilon = 0.01m^2/s$ and we will consider the ice phase to have $G = 10^9 Pa$, $\upsilon = 15m^2/s$. This choice of υ for the ice phase was chosen so that the attenuation rate for "pure ice" would be on the same order as those measured for high concentrations of ice in [14]. We will also consider $G = 10^7 Pa$ for the ice as the value of 10^9 is technically associated with solid, thick first year ice. In the MIZ, the ice tends to be thinner and well soaked with a lower freeboard making it more pliable. This is especially true near the edge and very characteristic of pancake ice. The value of $G = 10^7 Pa$ produces tighter bounds than that of $G = 10^9$, measurements would be required to nail down this parameter. The bounds for $G = 10^7 Pa$ are shown in Figure where we plot the complex conjugate of ν^* to better highlight the contrast in parameters. In reality the bounds are reflected over the real axis.

MATRIX PARTICLE ASSUMPTION

The bounds presented in the previous section can be improved by the calculation of higher moments, however this can prove difficult and the high contrast in parameters would require the calculation of several moments to see significant improvement. However, we may take advantage of a unique geometric property of the typical ice fields near the ice edge, particularly in pancake ice fields. Specifically, we may think of the ice floes as separated inclusions, with viscoelasticity ν_1, embedded in matrix of viscoelasticity ν_2. With this assumption, and some others described below, the supports of the measures μ and η in (10) can be restricted which provides tighter bounds. The further the separation of the particles, the larger the restriction on the support can made. The improved matrix particle bounds can be derived by following the work in [11] in which Golden extended the work of Bruno [5] where matrix particle bounds were derived for composites with components having real permitivity to that of complex permitivity. The quasi-static equations used in the electric case in [11] are essentially the same as the case of complex viscoelasticity here, and once the necessary assumptions for the electric case can be satisfied with the viscoelastic case, the same calculations are possible. In the viscoelastic case the displacement u plays the role of the electric potential function.

First we describe the composite in a slightly different way than in the previous section. Consider a material occupying a unit square $\Lambda \in \mathbb{R}^2$ with a corner at the origin. We necessarily assume that the square Λ is much larger than the size of the ice inclusions. In our particular case we consider a square where the "upper" surface is at a wave crest and the "lower" is at a point halfway between the crest and the trough, where the wave is at zero displacement, highlighting how important the long wavelength, slow moving condition is. This is to provide a physical setting for the for the following conditions. We require that along the upper surface, $u = 1$ while on the lower surface $u = 0$. We further require that the partial derivative of the u in the direction normal to the side walls ($\partial_n u$) be zero. Since we are assuming a plane wave, along the side walls the displacement does not change in the direction transverse to the wave propagation, ensuring a zero partial derivative in that direction. Together with (4), we further require that u be harmonic inside the inclusions and out. We have this condition since $\nabla \cdot u = 0$ and because $\Lambda_{s_{ijkl}} \epsilon_{kl} = 2\epsilon_{ij}$, we can say that $0 = \nabla \cdot \sigma = \nabla \cdot \nu^* \Lambda_{s_{ijkl}} \epsilon_{kl} = 2\nu^* \nabla^2 u$.

With the above conditions satisfied, we can carry forward the calculations in [11] and find that the support of the measure μ in (10) for $F(S)$ can be restricted to the interval $s_m \leq \lambda \leq S_M$ where the endpoints of the interval are given by

$$s_m = \frac{1}{2}(1 - q^2)\,, \qquad s_M = \frac{1}{2}(1 + q^2)\,. \tag{16}$$

Here, q is the separation parameter and is the ratio of the radius of the inclusion (r_i) to the largest circle that can be drawn before touching another inclusion (r_0). With the restricted measures the Stieltjes intergals in (10) become,

$$F(s) = \int_{s_m}^{s_M} \frac{d\mu(\lambda)}{s - \lambda}\,, \qquad E(s) = \int_{s_m}^{s_M} \frac{d\eta(\lambda)}{s - \lambda}\,. \tag{17}$$

If we then let $s = (S_M - s_m)t + s_m$ our restricted interval is mapped to $(0, 1)$ in the $t-$plane. This yields alternate Stieltjes integrals,

$$H(s) = \int_0^t \frac{d\mu^{mp}(\lambda)}{t-\lambda}, \qquad G(t) = \int_0^1 \frac{d\eta^{mp}(\lambda)}{t-\lambda}, \quad (18)$$

where the new measures have masses

$$\mu_0^{mp} = \frac{p_1}{s_m - s_m}, \qquad \eta_0^{mp} = 1 - \frac{p_1}{s_M - s_m}. \quad (19)$$

Following the same procedure to derive the bounds as in the elementary case, by fixing the masses above, we find that ν^* must lie with in the circular arcs,

$$K = \frac{p_1}{s - ((s_M - s_m)\lambda + s_m)}, \quad (20)$$

$$\hat{K} = \frac{p_1(s - s_m) - (s_M - s_m)^2\lambda}{(s - s_m)(p_1 + s - s_M) - (s_M - s_m)^2\lambda}. \quad (21)$$

for $-\infty \leq \lambda \leq \infty$. Here, K does not provide any additional improvement and coincides with Q. However $\hat{K}$ is an improvement over $\hat{Q}$ providing much tighter bounds and intersects with K at the points $\nu_2(1 - \hat{K}(0))$ and $\nu_2(1 - K(0))$. The bounds themselves are shown in Figure , along with laboratory data obtained in a wave tank with filled with densely packed pancake ice [26]. The data was taken specifically for the model presented in [25], which corresponds to our governing equations. In Figure , we take $q = 0.9$, $p_1 = 0.9$ which are representative of a closely packed and dense pancake ice field, with constituent parameters $G_1 = 10^7$, $G_2 = 0$, $\upsilon_1 = 5$, and $\upsilon_2 = 0.01$. For these values, we capture the laboratory data obtained for the model in [25]. The bounding arcs lie on top of each other giving a relatively small range of viscosity, the imaginary component, values and provides a vast improvement over the elementary bounds. We note that the range of values for the real component, effective shear modulus, remains relatively large but provides an order of magnitude better bound.

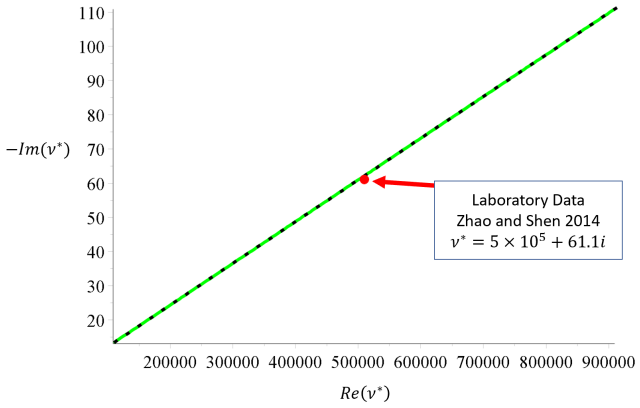

FIG. 2. The matrix particle bounds which apply to the pancake ice case. Here the intersection of the improved arc Q_m and previous arc $\hat{Q}$ essentially lie on top of each other in the imaginary, viscosity, component but vary over a wide set of bulk modulus, real, component.

CONCLUSION

We have derived the first bounds for the effective viscoelasticity of an ice covered ocean which depends only on the geometry of the ice-slush composite. The high contrast in constituent parameters produces elementary bounds with wide range, however under the matrix particle assumption the bounds are greatly improved. These particular bounds depend only on knowledge of the constituent parameters and the relative volume fractions of each enabling for the rapid determination of the effective parameter based on limited knowledge of ice geometry and concentration. We hope this can have wide application in modeling wave propagation through the marginal ice zone.

* golden@math.utah.edu

[1] Howard F. Bates and Lewis H. Shapiro. Long-period gravity waves in ice-covered sea. *Journal of Geophysical Research*, 85(C2):1095, 1980.

[2] David J Bergman. Rigorous bounds for the complex dielectric constant of a two-component composite. *Annals of Physics*, 138(1):78–114, jan 1982.

[3] Carlos Bonifasi-Lista and Elena Cherkaev. *Identification of Bone Microstructure from Effective Complex Moduls*, pages 91–96. Springer Netherlands, Dordrecht, 2007.

[4] Carlos Bonifasi-Lista and Elena Cherkaev. Analytical relations between effective material properties and microporosity: Application to bone mechanics. *International Journal of Engineering Science*, 46(12):1239–1252, dec 2008.

[5] O. Bruno. Effective moduli of strongly heterogeneous composites. In G.Bouchitté, G.Butazzo, and P.Suquet, editors, *Calculus of Variations, Homogenization and Continuum Mechanics*, pages 99–115. World Scientific, 1994.

[6] Oscar P. Bruno and Perry H. Leo. On the stiffness of materials containing a disordered array of microscopic holes or hard inclusions. *Archive for Rational Mechanics and Analysis*, 121(4):303–338, 1993.

[7] Elena Cherkaev and Carlos Bonifasi-Lista. Characterization of structure and properties of bone by spectral measure method. *Journal of Biomechanics*, 44(2):345–351, jan 2011.

[8] GF Dell'Antonio, R Figari, and E Orlandi. An approach through orthogonal projections to the study of inhomogeneous or random media with linear response. In *Annales de l'IHP Physique théorique*, volume 44, pages 1–28, 1986.

[9] K. Golden. Bounds on the complex permittivity of a multicomponent material. *Journal of the Mechanics and Physics of Solids*, 34(4):333–358, jan 1986.

[10] K. Golden and G. Papanicolaou. Bounds for effective parameters of heterogeneous media by analytic continuation. *Communications in Mathematical Physics*, 90(4):473–491, dec 1983.

[11] K. M. Golden. The interaction of microwaves with sea ice. In G. Papanicolaou, editor, *Wave Propagation in Complex Media, IMA Volumes in Mathematics and its Applications, Vol. 96*, pages 75 – 94. Springer – Verlag, 1997.

[12] Joseph B. Keller. Gravity waves on ice-covered water. *Journal of Geophysical Research: Oceans*, 103(C4):7663–7669, apr 1998.

[13] A. L. Kohout, M. J. M. Williams, S. M. Dean, and M. H. Meylan. Storm-induced sea-ice breakup and the implications for ice extent. *Nature*, 509(7502):604–607, may 2014.

[14] Alison L. Kohout, Michael H. Meylan, and David R. Plew. Wave attenuation in a marginal ice zone due to the bottom roughness of ice floes. *Annals of Glaciology*, 52(57):118–122, may 2011.

[15] G. W. Milton. Bounds on the complex permittivity of a two-component composite material. *Journal of Applied Physics*, 52(8):5286–5293, aug 1981.

[16] G.W. Milton. *The Theory of Composites*. Cambridge Monographs on Applied and Computational Mathematics. Cambridge University Press, 2002.

[17] Johannes E. M. Mosig, Fabien Montiel, and Vernon A. Squire. Comparison of viscoelastic-type models for ocean wave attenuation in ice-covered seas. *Journal of Geophysical Research: Oceans*, 120(9):6072–6090, sep 2015.

[18] N. Benjamin Murphy, Elena Cherkaev, Christel Hohenegger, and Kenneth M. Golden. Spectral measure computations for composite materials. *Communications in Mathematical Sciences*, 13(4):825–862, 2015.

[19] Karl Newyear and Seelye Martin. Comparison of laboratory data with a viscous two-layer model of wave propagation in grease ice. *Journal of Geophysical Research: Oceans*, 104(C4):7837–7840, apr 1999.

[20] Miao-Jung Ou and Elena Cherkaev. On the integral representation formula for a two-component elastic composite. *Mathematical Methods in the Applied Sciences*, 29(6):655–664, 2006.

[21] G.W. Timco and W.F. Weeks. A review of the engineering properties of sea ice. *Cold Regions Science and Technology*, 60(2):107–129, feb 2010.

[22] S Tokarzewski, JJ Telega, and A Gałka. Torsional rigidities of cancellous bone filled with marrow: The application of multipoint pads approximants. *Engineering Transactions*, 49(2-3):135–153, 2001.

[23] S Torquato and HW Haslach. Random heterogeneous materials: Microstructure and macroscopic properties. *Applied mechanics reviews*, 55(4):B62–B63, 2002.

[24] P. Wadhams. SAR imaging of wave dispersion in Antarctic pancake ice and its use in measuring ice thickness. *Geophysical Research Letters*, 31(15), 2004.

[25] Ruixue Wang and Hayley H. Shen. Gravity waves propagating into an ice-covered ocean: A viscoelastic model. *Journal of Geophysical Research*, 115(C6), June 2010.

[26] Xin Zhao and Hayley H. Shen. Wave propagation in frazil/pancake, pancake, and fragmented ice covers. *Cold Regions Science and Technology*, 113:71–80, may 2015.